Geodesy and Geodynamics 8 (2017) 377–388

Contents lists available at ScienceDirect

Geodesy and Geodynamics

journal homepages: www.keaipublishing.com/en/journals/geog;
http://www.jgg09.com/jweb_ddcl_en/EN/volumn/home.shtml

Improved geophysical excitations constrained by polar motion observations and GRACE/SLR time-dependent gravity

Wei Chen [a, b, *], Jiancheng Li [a], Jim Ray [c, 1], Minkang Cheng [b]

[a] Collaborative Innovation Center of Geospatial Technology/Key Laboratory of Geospace Environment and Geodesy, School of Geodesy and Geomatics, Wuhan University, China
[b] Center for Space Research, University of Texas at Austin, USA
[c] National Oceanic and Atmospheric Administration, Silver Spring, MD, USA

ARTICLE INFO

Article history:
Received 23 March 2017
Accepted 26 April 2017
Available online 5 June 2017

Keywords:
Polar motion
GRACE
SLR
Least difference combination
Atmospheric, oceanic, and hydrological/crospheric excitation

ABSTRACT

At seasonal and intraseasonal time scales, polar motions are mainly excited by angular momentum fluctuations due to mass redistributions and relative motions in the atmosphere, oceans, and continental water, snow, and ice, which are usually provided by various global atmospheric, oceanic, and hydrological models (some with meteorological observations assimilated; e.g., NCEP, ECCO, ECMWF, OMCT and LSDM etc.). Unfortunately, these model outputs are far from perfect and have notable discrepancies with respect to polar motion observations, due to non-uniform distributions of meteorological observatories, as well as theoretical approximations and non-global mass conservation in these models. In this study, the LDC (Least Difference Combination) method is adopted to obtain some improved atmospheric, oceanic, and hydrological/crospheric angular momentum (AAM, OAM and HAM/CAM, respectively) functions and excitation functions (termed as the LDCgsm solutions). Various GRACE (Gravity Recovery and Climate Experiment) and SLR (Satellite Laser Ranging) geopotential data are adopted to correct the non-global mass conservation problem, while polar motion data are used as general constraints. The LDCgsm solutions can reveal not only periodic fluctuations but also secular trends in AAM, OAM and HAM/CAM, and are in better agreement with polar motion observations, reducing the unexplained excitation to the level of about 5.5 mas (standard derivation value; about 1/5–1/4 of those corresponding to the original model outputs).

1. Introduction

Polar motion excitation involves the mass redistributions and motions within the Earth system relative to the mantle, as well as the Earth's responses to these perturbations [1–5]. At seasonal and intra-seasonal time scales, mass redistributions and relative motions are dominated by changes in the Earth's fluid envelopes, namely, the atmosphere, oceans, and continental water, snow and ice [5–13]. These changes cause fluctuations of the atmospheric, oceanic and hydrological angular momenta (AAM, OAM and HAM, respectively), and therefore lead to opposing changes of the angular momentum of the solid Earth, and hence excite polar motions.

Several versions of the AAM, OAM and HAM time series are calculated on the basis of GCMs (general circulation models) for numerical weather prediction developed at various institutes (see Table 1). The theories, numerical methods and assumptions adopted by the different institutes sometimes differ, so their global atmospheric, oceanic and hydrological model outputs are not identical (see Appendix A for some details). In addition, concerning the combined effects of atmospheric, oceanic and hydrological excitations (AE, OE and HE, respectively), we cannot simply add arbitrary versions of OE and HE to a certain AE since consistency

* Corresponding author. Collaborative Innovation Center of Geospatial Technology/Key Laboratory of Geospace Environment and Geodesy, School of Geodesy and Geomatics, Wuhan University, China.
E-mail address: wchen@sgg.whu.edu.cn (W. Chen).
Peer review under responsibility of Institute of Seismology, China Earthquake Administration.
[1] Retired.

Production and Hosting by Elsevier on behalf of KeAi

http://dx.doi.org/10.1016/j.geog.2017.04.006

Table 1
Basic information for some model outputs.

Model(s)/Data	Product(s)	Availability[a]
NCEP/NCAR	AAM and HAM (reanalysis)	Available since 1948
ECCO	OAM	Depends on version[b]
ECMWF	AAM (ERA40, ERAinterim, operational)	ERA40: available from 1958 to 2001
OMCT	OAM (ERA40, ERAinterim, operational)	ERAinterim: available since 1989
LSDM	HAM (ERA40, ERAinterim, operational)	operational: available since 2000

[a] According to the websites of the IERS Special Bureaus for Atmosphere, Ocean and Hydrology.
[b] The kf080g run adopted in this study is available since 1993; the original anomalous trend in the kf80 run since 2012 has been corrected in this version.

among these atmospheric, oceanic and hydrological models would not be ensured. That is, the models of the ocean and hydrology should be the ones driven by outputs from the same atmosphere model [5]. Artificial signals might be introduced if modeling consistency is not enforced.

In addition, due to non-uniform and sparse distributions of observatories and limitations in those models, the output atmospheric, oceanic and hydrological data still contain large uncertainties. As to the limitations in the GCMs, here we only provide two examples:

1. The hydrostatic equation adopted by the atmosphere models gives the relation between the air density and the decrease of pressure with height. However, it is only an approximation of the real atmosphere, valid for horizontal scales larger than a few tens of kilometers [14].
2. In many cases, the atmosphere, ocean and hydrology models are developed in a somewhat independent manner and thus the global (atmospheric, oceanic and hydrological) mass is not conserved [15].

Koot et al. [16] estimated the noise levels of various AAMs and constructed a combined AAM series using time-dependent weights chosen so that the noise level of the combined series is minimal. Neef and Matthes [17] compared atmospheric model simulations with and without meteorological data constraints, and identified the potential for the assimilation of ERPs (Earth Rotation Parameters) as an additional constraint on atmospheric models. Gross [3] concluded that a rather large residual remains after the effects of the atmosphere and oceans are removed from the observed seasonal polar motion excitation. Brzeziński et al. [11] and Chen et al. [5] further showed that including hydrological models hardly helps to reduce the residual and the residual is mostly caused by errors in the atmospheric, oceanic and hydrological models, due to the model limitations mentioned above. Chen et al. [5] proposed a LDC (Least Difference Combination) method (also see Section 3 for details), obtained the LDC1 and LDC2 AAMs, OAMs and HAMs by combining various model-based geophysical excitations, and showed that the differences (residuals) between the LDC1 (or LDC2) data set and the geodetic excitation are reduced significantly.

The time series of degree-2 tesseral geopotential coefficients (C_{21}, S_{21}) are directly linked to Earth's polar motion while the degree-2 zonal one C_{20} is closely related with variations in length of day. Only polar motion and (C_{21}, S_{21}) for an Earth model with frequency-dependent responses are considered in this study, and variations in length of day and C_{20} will be considered in another study with an improved theory for the excitations of length-of-day variations.

The 2002 launch of the GRACE (Gravity Recovery and Climate Experiment) twin satellites has made available several time series of geopotential coefficients. Meanwhile, SLR (Satellite Laser Ranging) also provides time-dependent low-degree geopotential coefficients by tracking the orbits of Starlette, LAGEOS-1/2 (Laser Geodynamics Satellites) and other satellites [18–20]. These GRACE and SLR measurements reflect mass transports in atmosphere, oceans, land water and cryosphere (as well as mostly slow variations within the solid Earth, such as glacial isostatic adjustment) and make it possible to handle the non-conservation problem in atmospheric, oceanic and hydrological models.

Nastula et al. [21] showed that GRACE-based excitations are in good agreement with the geodetic one. Brzeziński et al. [11] found that combination of the GRACE-derived mass term of excitation with the motion terms of atmospheric and oceanic excitations brings the excitation balance considerably closer in case of the retrograde/prograde annual and retrograde semiannual components of polar motion. Göttl et al. [22] developed an adjustment model to combine precise observations from GRACE/SLR and other space geodetic observation systems in order to separate geophysical excitation mechanisms of Earth rotation. However, Göttl et al. mistook the AOD1B GAA and GAB products as observations while they are only model outputs [23,24] (also see Section 3 of this study), which makes their results meaningless. In the present study, we intend to generalize the LDC method by assimilating GRACE/SLR data to obtain better understanding of atmospheric, oceanic and hydrological/cryospheric excitations of polar motion.

This paper is organized as follows: in Sections 2 and 3, we will describe the theoretical relation between geopotential coefficients (C_{21}, S_{21}) and polar motion excitations, as well as the data used, respectively; in Section 4, we will summarize the basic ideas and methods of using polar motion and GRACE/SLR (C_{21}, S_{21}) time-series to improve and correct the meteorological data, and present the main numerical results; finally, Discussions and Conclusions are in Section 5.

2. Theory

2.1. Liouville's equation and geophysical excitations

Theoretically, polar motion excitations are governed by the linearized Liouville's equation [1–4].

$$\frac{\mathrm{i}}{\sigma_{\mathrm{CW}}}\dot{p}+p=\chi,\quad \mathrm{i}=\sqrt{-1} \tag{1}$$

$$\chi=T^{\mathrm{L}}*\frac{c}{C-A}+T^{\mathrm{NL}}*\frac{h}{\Omega(C-A)} \tag{2}$$

where $\sigma_{\mathrm{CW}}=2\pi f_{\mathrm{CW}}(1+i/2Q_{\mathrm{CW}})$ is the complex Chandler frequency with its imaginary part accounting for dissipation, $p=x-\mathrm{i}y$ the coordinates of the CIP measured in the ITRF (International Terrestrial Reference Frame), C and A the Earth's polar and mean equatorial principal moments of inertia, and Ω the mean rotation rate of the Earth. As shown in Eq. (2), mass redistributions, c, and relative motions, h, drive the effective polar motion excitation function χ through the polar motion transfer functions T^{L} and T^{NL} (L and NL for with and without loading effects, respectively; * means convolution), which describe the responses of the stratified and deformable Earth. The transfer functions T^{L} and T^{NL} play significant roles in understanding the relationship between polar motion and the underlying geophysical processes associated with mass redistributions and relative motions, and are complex functions of frequency mantle anelasticity, quasi-fluid rheology, dynamic ocean tides and ocean pole tides [2,4].

The GCMs for atmosphere, ocean and hydrology provide the average temporal mass densities ρ and horizontal wind/current velocities (u, v) of the atmosphere, ocean and continental water within certain grids, and thus the excitations for the matter and motion terms can be determined by Refs. [25–28].

$$\chi^{\text{matter}} = T^{\text{L}} * \frac{c}{C-A}, \quad c = -\int_V \rho r^2 \sin\theta \cos\theta e^{i\lambda} \mathrm{d}V \tag{3}$$

and

$$\chi^{\text{motion}} = T^{\text{NL}} * \frac{h}{\Omega(C-A)}, \quad h = -\int_V \rho r(u \sin\theta + iv) e^{i\lambda} \mathrm{d}V \tag{4}$$

Using the atmosphere, ocean and hydrology data provided by the above-mentioned institutes (also see Table 1), the matter terms (Ωc) and motion terms (h) of AAMs, OAMs and HAMs are calculated and released by the IERS Special Bureaus of Atmosphere, Ocean and Hydrology.

For GRACE and SLR degree-2 tesseral potential coefficients, mass redistributions c can be derived by

$$(1+k')c = \sqrt{\frac{5}{3}} Ma^2 (\Delta C_{21} + \mathrm{i}\Delta S_{21}), \quad \mathrm{i} = \sqrt{-1} \tag{5}$$

as these potential coefficients reflect not only mass redistributions but also the associated loading deformations of the Earth [3,29]. In Eq. (5), k' is the degree-2 order-1 load Love number, M and a are the mass and mean equatorial radius of the Earth, respectively.

2.2. Dynamic equations in frequency domain

The frequency domain expression for the effective polar motion excitation χ can be written as [1–4,11,25,30].

$$\chi_{\text{matter}}(f) = T^{\text{L}}(f) \frac{c(f)}{C-A} \tag{6}$$

$$\chi_{\text{motion}}(f) = T^{\text{NL}}(f) \frac{h(f)}{\Omega(C-A)} \tag{7}$$

Using the consistent estimates of the fundamental Earth parameters in Chen et al. [31,4,32], $A = 8.0085964 \times 10^{37}$ kg m^2, $C = 8.0349010 \times 10^{37}$ kg m^2, and T^{L} and T^{NL} respectively take the values 1.141987−0.000056i and 1.660573 + 0.000044i for the weekly band, but 1.147018 + 0.000725i and 1.799738 + 0.009668i for the Chandler band. The imaginary parts of T^{L} and T^{NL} just reflect the effects of mantle anelasticity and dissipative oceanic dynamics [4,33]. Worth mention, relying on the 3-D displacement field observed by the GPS (Global Positioning System) and gravity variations from superconducting gravimeter records, Ding and Chao [34] determined the complex Love numbers at the Chandler band and provided an independent clue that the theory of Earth's frequency-dependent responses as presented by Chen et al. [4] is reliable.

From the first two equations of Eq. (18) in Chen et al. [32], the mean equatorial principal moment of inertia can be written as

$$A = -\sqrt{5} Ma^2 \frac{A_{20}}{e} \tag{8}$$

where $A_{20} = (4{,}841{,}694.6 \pm 0.2) \times 10^{-10}$ is the degree-2 zonal potential coefficient in the Earth's principal axes system [31,32,35], and $e = (C-A)/A$ is the dynamic ellipticity of the Earth.

Inserting Eqs. (5) and (8) into Eq. (6) and noting $T^{\text{L}} = (1+k')\,T^{\text{NL}}$, the matter-term excitation for GRACE or SLR can be written in a form related only to the transfer function and the potential coefficients:

$$\chi_{\text{matter}}(f) = -\frac{T^{\text{NL}}(f)}{\sqrt{3}} \frac{CS(f)}{A_{20}} \tag{9}$$

where $CS(f)$ is the Fourier transformation of $\Delta C_{21}(t) + \mathrm{i}\Delta S_{21}(t)$. One advantage of using Eq. (9) is that we can calculate the matter-term excitations directly from the GRACE and SLR potential coefficients; another and more important advantage is that we can avoid using Earth's mass M or principal moment of inertia A, which still suffer from large uncertainties [32,36].

In order to validate the geophysical excitations, we need to convert the polar motion data to the geodetic or observed excitation using the frequency-domain expression of the Liouville's equation [37].

$$\chi_{\text{obs}}(f) = \frac{\sigma_{\text{CW}} - 2\pi\mathrm{f}}{\sigma_{\text{CW}}} p(f) \tag{10}$$

After applying the above equations to relevant data in the frequency domain, we can use the inverse Fourier transformation to convert the frequency-domain results to time-domain ones.

3. Data

This study needs various data sets, which are listed in Tables 2 and 3.

In Table 2:

- The IERS EOP 08 C04 (IAU2000A version) [38] provides the Earth's orientation parameters within the reference frame ITRF2008. The polar motion series contained in this data file is used as the reference and verifying data in establishing the “optimized” atmospheric, oceanic and hydrological/cryospheric excitations.
- The GRACE GSM RL05 (RL05 means release 05) provides gravity field solutions with modeled atmosphere and ocean contributions removed (see below). The GRACE monthly geopotential models from JPL (Jet Propulsion Laboratory), CSR (Center for

Table 2
Data used.

Data	Version(s)	Availability
IERS EOP 08 C04	IAU2000A	Since 1962 from IERS website
GRACE GSM RL05	CSR, GFZ, JPL	Since 2002 from ftp://podaac-ftp.jpl.nasa.gov/
GRACE GAC RL05	CSR, GFZ, JPL	Since 2002 from ftp://podaac-ftp.jpl.nasa.gov/
SLR potential coefficients[a]	15-day solution	Since 1979 from M.K. Cheng
SLR potential coefficients[a]	30-day solution	Since 1993 from M.K. Cheng

[a] No AOD1B data are used in the two special runs of SLR potential coefficients.

Table 3
Meteorological model/data sets used in this study.

Model/Data Set	Product(s)
NCEP	NCEP/NCAR AAM (reanalysis) + ECCO OAM[a]
ECMWFop	ECMWFop AAM + OAM + HAM
ERAinterim	ERAinterim AAM + OAM + HAM
LDCgsm	LDCgsm AAM + OAM + HAM[b]

[a] The NCEP HAM is not used due to its very poor accuracy. Adding NCEP HAM will only degrade the quality of the NCEP data set [5].
[b] The LDCgsm solutions are constructed in Section 4 of this study.

Space Research) and GFZ (GeoForschungsZentrum) are all used in this study.

- The GRACE GAC RL05 is a subset of GRACE AOD1B (Atmosphere and Ocean Level-1B De-Aliasing) Product, which is intended to provide a model-based data-set that describes the time variations of the gravity potential at satellite altitudes that are caused by non-tidal mass variability in the atmosphere and oceans. GAC describes the sum of monthly non-tidal atmospheric and oceanic mass anomalies simulated by the operational run of the atmosphere model ECMWF and the (unconstrained) ocean model OMCT [23,24]. Therefore, GSM + GAC is what GRACE satellites really measure.

Due to the upgrades of horizontal and vertical resolutions in the ECMWF model, the GAC data contain the following two notable jumps [24,39]:

1) between 2006-01-29 18 h and 2006-01-30 00 h
2) between 2010-01-26 00 h and 2010-01-26 06 h

Which would cause opposite jumps in the GSM data. Also taking into account that AOD1B data are derived from the ECMWF and OMCT operational outputs, which are far from perfect as shown in a detailed analysis by Chen et al. [5], it would be better to add AOD1B back to the GRACE data, namely using GSM + GAC instead of using GSM alone. In this study, we always mean GSM + GAC when we mention GRACE data.

- Two special runs of SLR data provided by M.K. Cheng: one sampled every 15 days from 1979 to 2015, the other sampled every month from 1993 to 2015, both customized not to use AOD1B correction. Thus they are suitable to describe the mass transportations of the Earth system, including atmosphere and oceans.

The long-period pole tide corrections recommended by Wahr et al. [40] are applied to all the GRACE and SLR data, which eliminate most of the divergences in their trends. All GRACE and SLR data are interpolated with a cubic spline to daily sampling and then filtered to remove the components outside of [−6, +6] cpy (cycles per year), which are totally caused by interpolation and have no geophysical meaning.

As shown in Table 3, we have also used the AAM, OAM and HAM time series derived from NCEP (National Centers for Environmental Prediction)/NCAR (National Center for Atmospheric Research, ECCO (Estimating the Circulation and Climate of the Ocean), ECMWF (European Centre for Medium-Range Weather Forecasts), OMCT (Ocean Model for Circulation and Tides) and LSDM (Land Surface Discharge Model). Except for daily-sampled ECCO OAM and all HAMs, all AAMs and OAMs are sampled every 6 h and thus should be down sampled to daily ones with a lowpass filter.

The ECCO ocean model is driven by the NCEP/NCAR atmosphere outputs [41], and thus NCEP/NCAR and ECCO are a consistent set (denoted simply as NCEP). OMCT and LSDM are both driven by the ECMWF atmosphere outputs, but the latter has many versions, such as the operational run ECMWFop and the interim reanalysis ERAinterim (the ERA40 data are out of the time-range of GRACE data and thus not used) [13]. Therefore, we have another two consistent data sets ECMWFop and ERAinterim (both together with OMCT and LSDM) where the driving model is used to name the data sets.

To match the resolution and time range of GRACE data, all other series listed in Tables 2 and 3 are filtered to keep components within [−6, +6] cpy and then truncated to range from Apr. 2002 to Dec. 2014.

4. Method and results

4.1. Least difference combination of GRACE/SLR data

First of all, let us summarize the basic idea for LDC (Least Difference Combination) method proposed by Chen et al. [5]:

Apply the FFT (Fast Fourier Transformation) to the time series of the reference data (REF) and the data/models to be combined (MOD), and get their FFT coefficients $a_{\mathrm{dat}}(f)$ and $b_{\mathrm{dat}}(f)$ corresponding to an arbitrary frequency f, where dat = REF, or MOD-K ($1 \le K \le N$, where N is the number of the data/model sets to be combined). Those coefficients carry all the information about the amplitude and phase of the data component for the frequency f (note that $\sqrt{a^2_{\mathrm{dat}}(f) + b^2_{\mathrm{dat}}(f)}$ and $b_{\mathrm{dat}}(f)/a_{\mathrm{dat}}(f)$ are respectively the amplitude and the tangent of phase angle for this component). Therefore, we can construct a combined data set by gathering all the frequency components from MOD closest to the REF in terms of FFT coefficients, namely

$$\begin{aligned}
&a_{\mathrm{LDC}}(f) = a_{\mathrm{REF}}(f) - \mathrm{Res}a_{\mathrm{LDC}}(f)\\
&b_{\mathrm{LDC}}(f) = b_{\mathrm{REF}}(f) - \mathrm{Res}b_{\mathrm{LDC}}(f)\\
&|\mathrm{Res}a_{\mathrm{LDC}}(f)| = \min\{|\mathrm{Res}a_{\mathrm{MOD-1}}(f)|,\\
&\qquad |\mathrm{Res}a_{\mathrm{MOD-2}}(f)|,\ \ldots,\ |\mathrm{Res}a_{\mathrm{MOD-N}}(f)|\}\\
&|\mathrm{Res}b_{\mathrm{LDC}}(f)| = \min\{|\mathrm{Res}b_{\mathrm{MOD-1}}(f)|,\\
&\qquad |\mathrm{Res}b_{\mathrm{MOD-2}}(f)|,\ \ldots,\ |\mathrm{Res}b_{\mathrm{MOD-N}}(f)|\}\\
&\mathrm{Res}a_{\mathrm{MOD}}(f) = a_{\mathrm{REF}}(f) - a_{\mathrm{MOD}}(f)\\
&\mathrm{Res}b_{\mathrm{MOD}}(f) = b_{\mathrm{REF}}(f) - b_{\mathrm{MOD}}(f)
\end{aligned} \tag{11}$$

and then apply the inverse FFT to a_{LDC} and b_{LDC} to obtain the LDC series. Special attention should be paid to the signs of $\mathrm{Res}a_{\mathrm{LDC}}(f)$ and $\mathrm{Res}b_{\mathrm{LDC}}(f)$: supposing $\mathrm{Res}a_{\mathrm{MOD-K}}(f)$ $(1 \le K \le N)$ has the smallest absolute value, then the sign of $\mathrm{Res}a_{\mathrm{LDC}}(f)$ is the same as that of $\mathrm{Res}a_{\mathrm{MOD-K}}(f)$; likewise for $\mathrm{Res}b_{\mathrm{LDC}}(f)$. One can see the LDC method can provide a good handle of both the magnitude and phase aspects simultaneously when combining different model data, and can be applied to any frequency f (including the lowest frequency component which is usually called the trend of a series), which is only limited by the sampling interval and length of a series. Therefore, the LDC method can also properly handle the trends and very-low frequency components of data, which is another important advantage of LDC over many other data combining or assimilation methods.

In many cases, various models are developed to explain some specific phenomenon (or observation). However, models are usually not in perfect agreement with observations, which is caused by the adopted approximations due to theoretical and/or practical reasons (see, e.g., the limitations of various atmospheric, oceanic and hydrological models as mentioned by Chen et al. [5] and Appendix A), and some model(s) may have better performance in some cases but worse one in other cases than other models. The parts not in good agreement with observations should be regarded as poorly modeled as observation with sufficient accuracy is the only criterion in judging models. Given the facts that limitations of various atmospheric, oceanic and hydrological models are inevitable [5,14,15] and the geodetic excitation is much more accurate than the geophysical excitations [42–44], it is natural to regard the frequency components of the geophysical models are well modeled if they agree with the geodetic excitation, and mismodeled if they have notable deviations with respect to the geodetic excitation. The well-modeled parts properly describe some real geophysical phenomena and should be retained while the mismodeled parts do not and thus should be discarded. Thus it is possible and meaningful to choose the best modeled components from each geophysical model and develop a hybrid model by “assembling” those parts. That is the physical meaning of the LDC method.

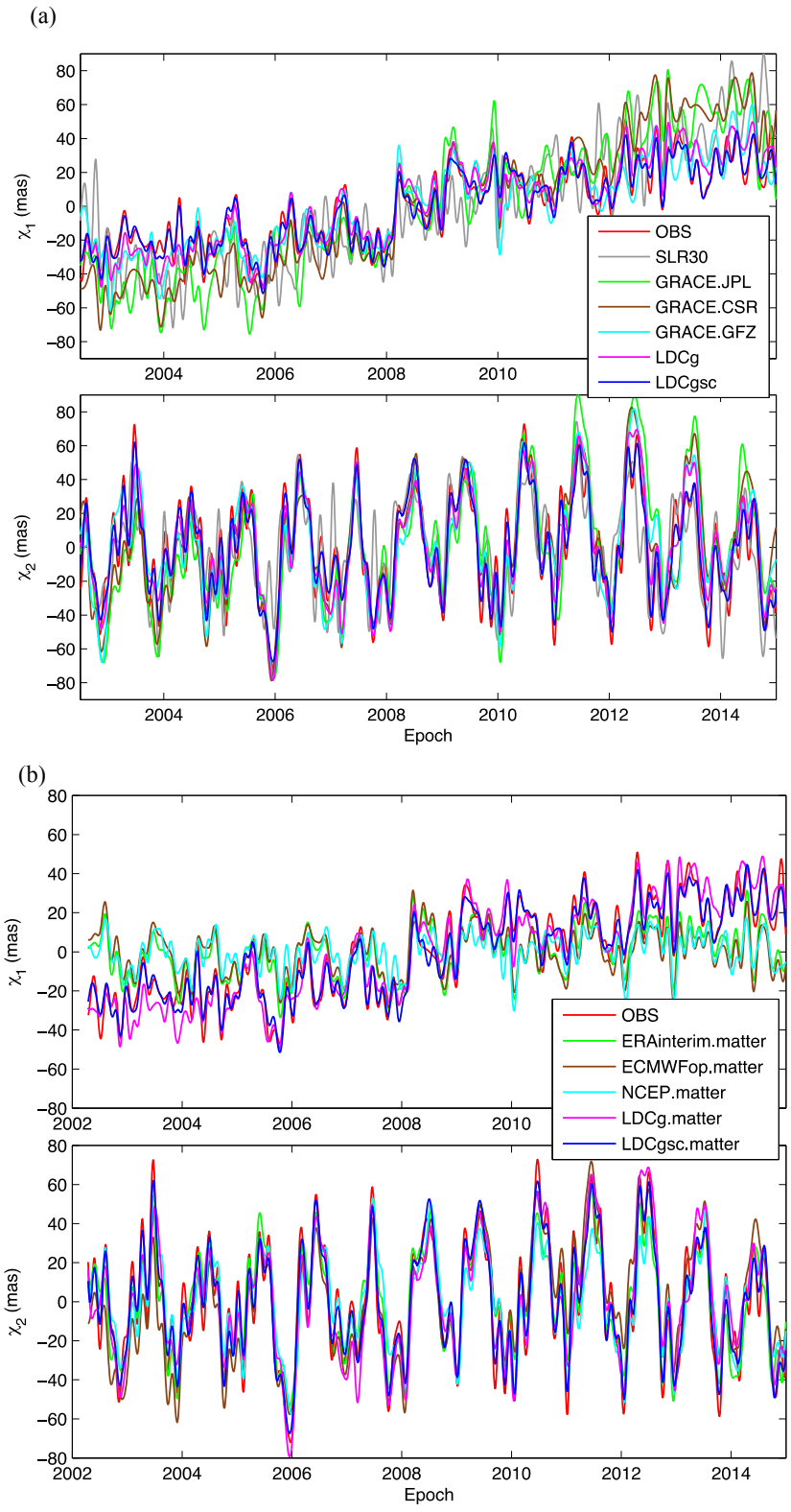

Fig. 1. Geodetic and matter-term excitations derived from various data/model sets. (a) The matter-term excitations from monthly GRACE and SLR potential coefficients (GSM + GAC) from the three main analysis centers, in comparisons with the geodetic (or observed) excitation derived from the IERS 08 C04 polar motion data. (b) The matter-term excitations from three meteorological data sets, in comparisons with the geodetic excitation. The combined solutions LDCg and LDCgsc are also displayed in both (a) and (b). We have used two special runs of SLR data provided by M.K. Cheng: the 15-day-interval data ranging from 1979 to 2015, and the monthly data ranging from 1993 to 2015, both including the contributions from atmosphere and oceans. Here we only show the plot of the 30-day-interval data since the two are quite close to each other. The long-period pole tide corrections to GRACE potential coefficients from Wahr et al. [40] have been applied to all the GRACE and SLR data. Only signals with frequencies within [−6, +6] cycles per year are kept for all data.

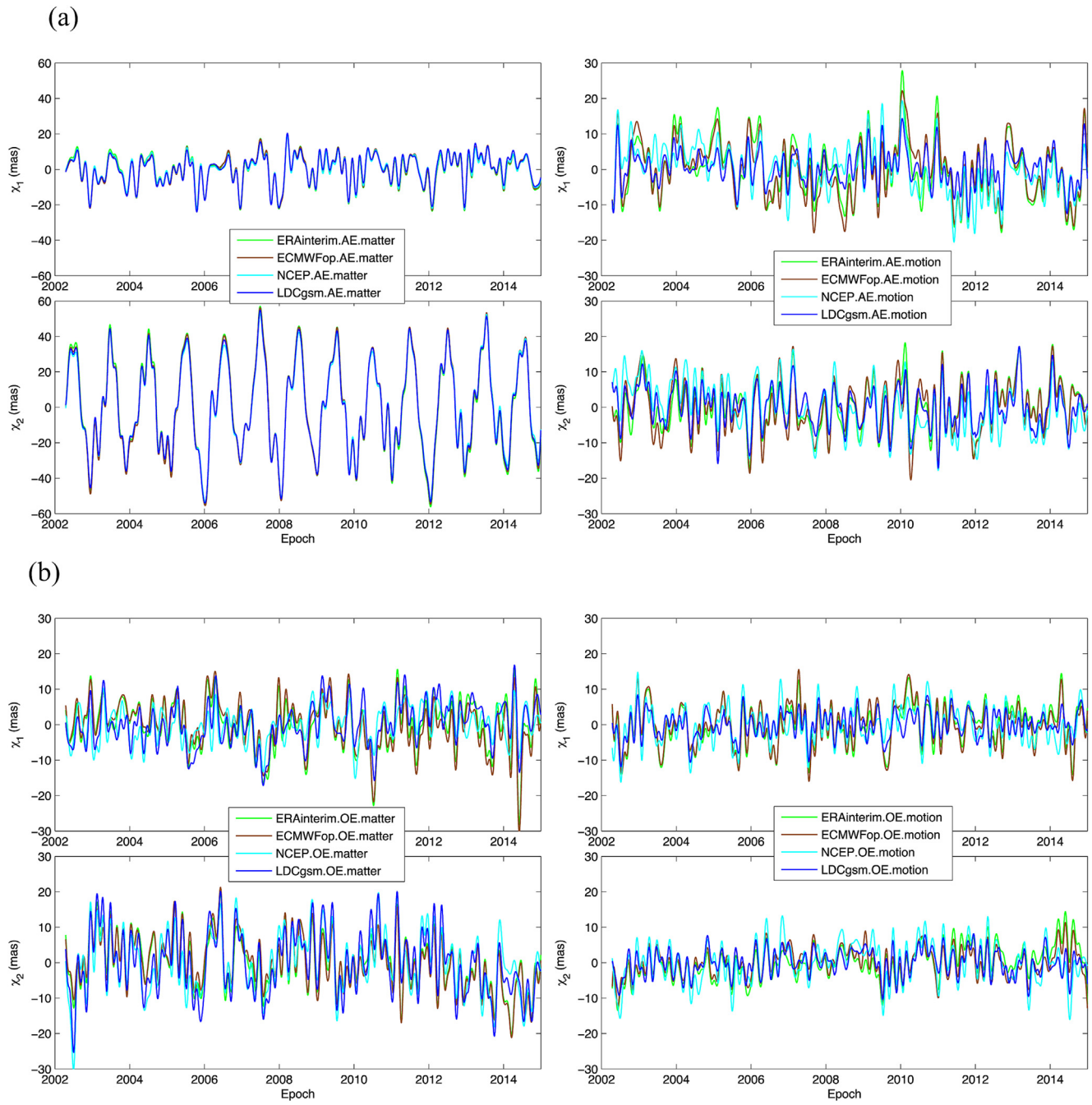

Fig. 2. Comparisons of the matter and motion terms of atmospheric, oceanic and hydrological excitations (AE, OE and HE, respectively) derived from various models and the LDCgsm combinations. Noting that GRACE and SLR also measure the changes in cryospheric mass, the LDCgsm HE/CE described in this study includes that part and is in fact a combination of hydrological and cryospheric excitations (CE). In addition, the hydrological models still contain quite large uncertainties. Therefore, it is not strange that LDCgsm HE/CE differs significantly from other HEs.

Among all the data described in Section 3, the geodetic excitation derived from polar motion data is of the highest quality [5,43,44]. Then, adopting the geodetic excitation as a reference, the LDC method can gather together all the frequency components that are closest to the geodetic excitation from the GRACE, SLR and meteorological data. The detailed steps are as follows:

1. Convert all the GRACE and SLR (C_{21}, S_{21}) to GRACE/SLR matter-term excitations according to Eq. (9). There are three (JPL, CSR and GFZ) versions of GRACE matter-term excitations, and two versions (15-day and 30-day) of SLR ones.
2. Apply the LDC method to combine all GRACE matter-term excitations, and obtain the combined GRACE-only solution $\chi^{\mathrm{LDCg}}_{\mathrm{matter}}$ denoted as LDCg; then add the SLR data and get another combination $\chi^{\mathrm{LDCgs}}_{\mathrm{matter}}$ denoted as LDCgs.
3. Apply LDC to the NCEP, ECMWFop and ERAinterim meteorological matter terms, and obtain the optimized matter-term meteorological excitation $\chi^{\mathrm{LDCm}}_{\mathrm{matter}}$ (namely the sum of AAM, OAM and HAM matter terms) denoted as LDCm.
4. Apply LDC again to $\chi^{\mathrm{LDCg}}_{\mathrm{matter}}$, $\chi^{\mathrm{LDCgs}}_{\mathrm{matter}}$ and $\chi^{\mathrm{LDCm}}_{\mathrm{matter}}$, and obtain the final solution $\chi^{\mathrm{LDCgsc}}_{\mathrm{matter}}$ denoted as LDCgsc, where “c” means the optimized meteorological data are introduced to correct the

(c)

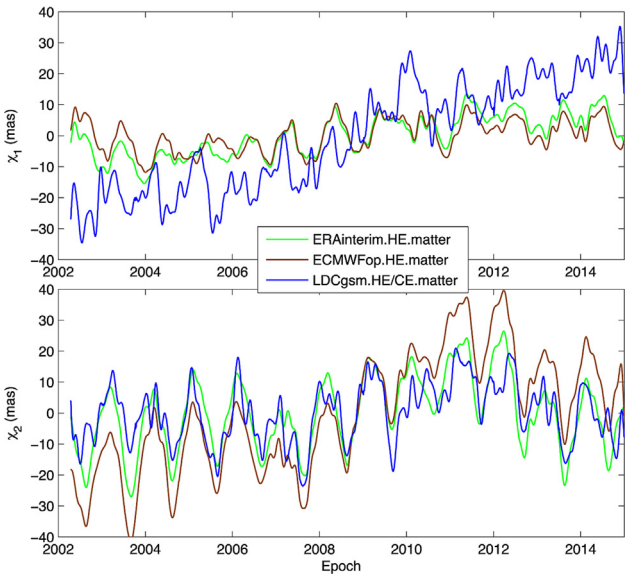

Fig. 2. (*continued.*)

unreasonable χ^{LDCgs}_{matter} components with frequencies higher than about 2 cpy.

The performance of χ^{LDCgsc}_{matter} is illustrated in Fig. 1, where one can see χ^{LDCgsc}_{matter} agrees best with the geodetic excitation, showing its obvious advantage over the original GRACE- and SLR-based excitations.

In the combination of χ^{LDCgsc}_{matter}, we have not removed the motion terms (derived from GCMs) from the geodetic excitation because doing so would bring no good but only degrade the accuracy of geodetic excitation as motion terms are poorly modeled (see Subsection 4.3 and Section 5 for more detailed discussions), and matter terms dominate polar motion excitations and are close enough to the geodetic excitation (Fig. 1).

In the following subsections, using χ^{LDCgsc}_{matter} and χ_{obs} as references, we can obtain the LDC matter and motion terms for AE, OE and HE/CE (atmospheric, oceanic and hydrological/cryospheric excitations, respectively; denoted as LDCgsm meteorological excitations) as done by Chen et al. [5].

4.2. Least difference combination of meteorological excitations

4.2.1. Steps to combine LDCgsm AE, OE and HE matter terms

1. Setting LDCgsc matter-term excitation χ^{LDCgsc}_{matter} as the REF and MOD = [NCEP AE.matter, ERAinterimAE.matter, ECMWFopAE.matter], using Eq. (11) we can obtain the optimized AE matter term, denoted as LDCgsm AE matter term $\chi^{LDCgsm}_{AE.matter}$;
2. Setting $\chi^{LDCgsc}_{matter} - \chi^{LDCgsm}_{AE.matter}$ as the REF and MOD = [NCEP OE.matter, ERAinterimOE.matter, ECMWFopOE.matter], using Eq. (11) we can obtain the optimized OE matter term, denoted as LDCgsm OE matter term $\chi^{LDCgsm}_{OE.matter}$;
3. Using $\chi^{LDCgsm}_{HE.matter} = \chi^{LDCgsc}_{matter} - \chi^{LDCgsm}_{AE.matter} - \chi^{LDCgsm}_{OE.matter}$ and getting the optimized HE matter term, denoted as LDCgsm HE matter term $\chi^{LDCgsm}_{HE.matter}$;

One can see $\chi^{LDCgsc}_{matter} \equiv \chi^{LDCgsm}_{matter} = \chi^{LDCgsm}_{AE.matter} + \chi^{LDCgsm}_{OE.matter} + \chi^{LDCgsm}_{HE.matter}$ and we have not applied LDC to ERAinterm HE and ECMWF HE since HEs are poorly modeled (Fig. 2) and the global mass must be conserved (noting that GRACE/SLR measure the total mass change). The LDCgsm motion-term excitations are used to validate the LDCgsc matter-term excitations in Figs. 3b and 4b.

4.2.2. Steps to combine LDCgsm AE, OE and HE motion terms

1. Setting $\chi_{OBS} - \chi^{LDCgsc}_{matter}$ as the REF and MOD = [NCEP AE.motion, ERAinterimAE.motion, ECMWFopAE.motion], using Eq. (11) we can obtain the optimized AE motion term, denoted as LDCgsm AE motion term $\chi^{LDCgsm}_{AE.motion}$;
2. Setting $\chi_{OBS} - \chi^{LDCgsc}_{matter} - \chi^{LDCgsm}_{AE.motion}$ as the REF and MOD = [NCEP OE.motion, ERAinterimOE.motion, ECMWFopOE.motion], using Eq. (11) we can obtain the optimized OE motion term, denoted as LDCgsm OE motion term $\chi^{LDCgsm}_{OE.motion}$;

One can refer to Figs. 2–4 and Table 4 for the time and frequency domain performances of the LDCgsm AE, OE and HE.

Using LDCg and geodetic excitation, the LGDCgm meteorological excitations can be generated in a similar way.

4.3. Comparisons in time and frequency domains

In Figs. 3 and 4, the LDCgsm motion-term excitations are used to validate the LDCgsc matter-term excitations (Noting that $\chi^{LDCgsc}_{matter} \equiv \chi^{LDCgsm}_{matter} = \chi^{LDCgsm}_{AE.matter} + \chi^{LDCgsm}_{OE.matter} + \chi^{LDCgsm}_{HE.matter}$ according to Subsection 4.2.1).

With the LDCgsm meteorological matter- and motion-term excitations (noting that the LDCgsc and LDCgsm matter term excitations are exactly the same), the excess excitation (the part of geodetic excitation unexplained by the sum of AE, OE and HE/CE) for LDCgsm reduces to less than 10 mas (milli-arc-seconds), while those for the original model sets are usually several times larger (Fig. 3). In addition, the power spectrum density (PSD) of LDCgsm is the closest to that of the geodetic excitation, and the excess excitation corresponding to LDCgsm has the lowest power (Fig. 4), implying the combined solution LDCgsm can significantly reduce the amplitudes of the unexplained excitations at all frequencies.

The statistical comparisons as listed in Table 4 can illustrate the significant improvements gained by the LDC serial solutions more quantitatively. The standard derivation of the excess excitation for LDCgsm is only 5.5 mas, while the numbers for the original model sets and GRACE/SLR-based data range from a minimal 20.5 mas to a maximal 32.8 mas (see Table 4 for more details).

Viewing Figs. 3 and 4 as well as Table 4, one can conclude that the LDCgsc and LDCgsm have overwhelming advantages in both time and frequency domains, relative to the original GRACE- and SLR-based excitations, the meteorological excitations derived from various climate models, and even the GRACE-only combination LDCg.

Ideally, there would be no excess excitation if the polar motion data and the matter- and motion-term excitations are perfectly observed and modeled. In practice, errors and uncertainties exist in the polar motion observations and geophysical modeling of mass changes and motions, thus there is some difference between χ_{obs} and $\chi_{matter} + \chi_{motion}$, known as the excess excitation χ_{excess}. Taking into account the high accuracy of polar motion observations, χ_{excess} is dominated by the uncertainties in χ_{matter} and χ_{motion}, and can be regarded as a measure of the qualities of models for mass changes and motions (such as meteorological models), and the accuracy of GRACE/SLR measurements.

From the spectrum analyses as shown by Fig. 4, it is clear that the GRACE and SLR data contribute more to the low-frequency components and the trends (especially after LDC combination, e.g., LGCg and LDCgsc), typically within ~[−2, +2] cpy, while all the climate models fail to model the secular trends. For components

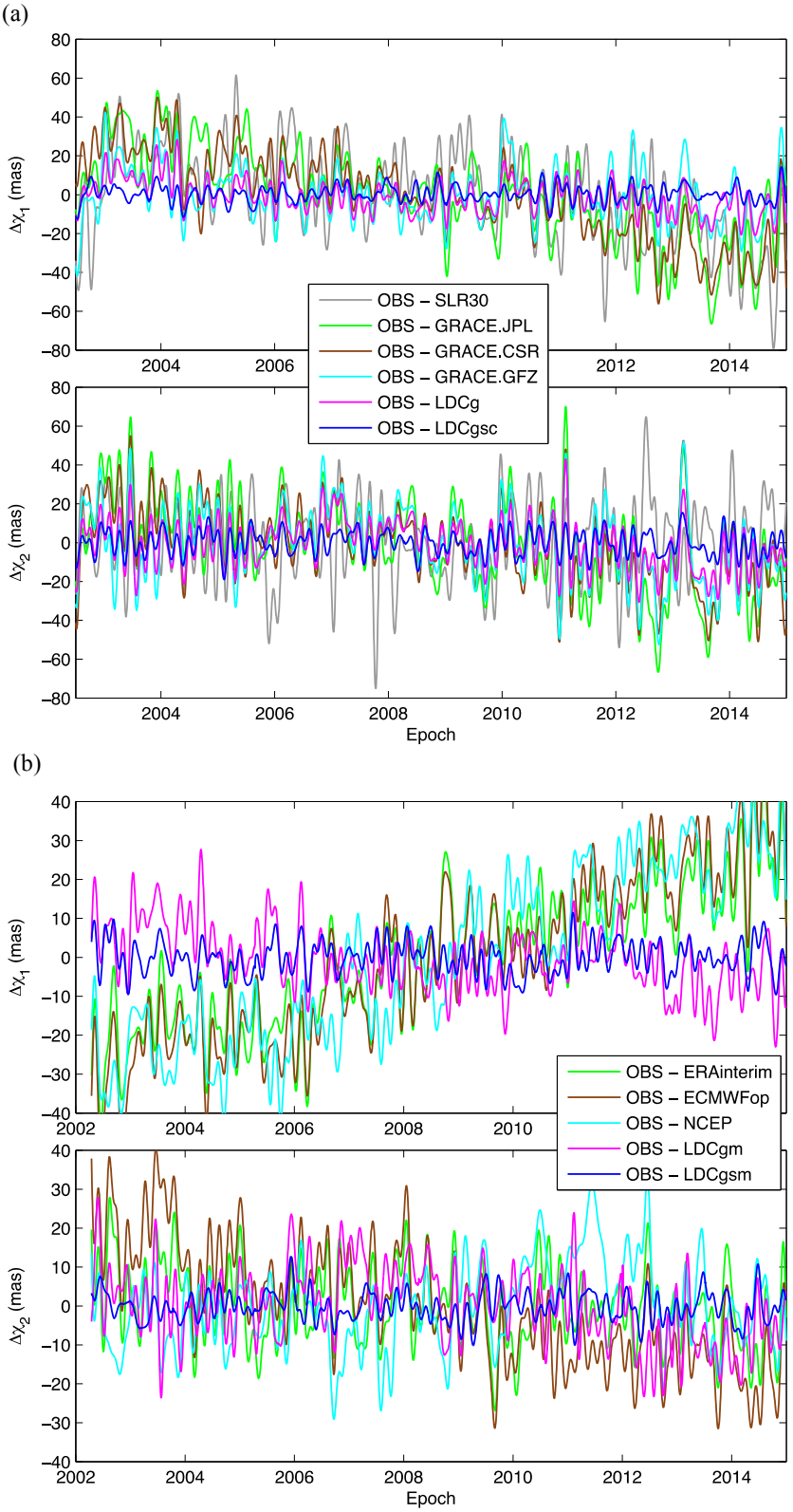

Fig. 3. The excess excitations unexplained by geophysical excitations. (a) Only matter-term excitations corresponding to various GRACE, SLR and LDC data are considered. The combined solutions LDCg and LDCgsc are much better than the original GRACE and SLR ones, reducing the amplitude of unexplained excitations to ~20 mas or less. By assimilating SLR data and meteorological matter terms, the LDCgsc solution has obvious advantage over the LDCg one. (b) Both matter-term and motion-term excitations corresponding to various atmospheric, oceanic and hydrological models as well as the combined solution LDCgsm are considered. The LDCgsm are much better than the original meteorological excitations, reducing the amplitude of unexplained excitations to ~10 mas or less.

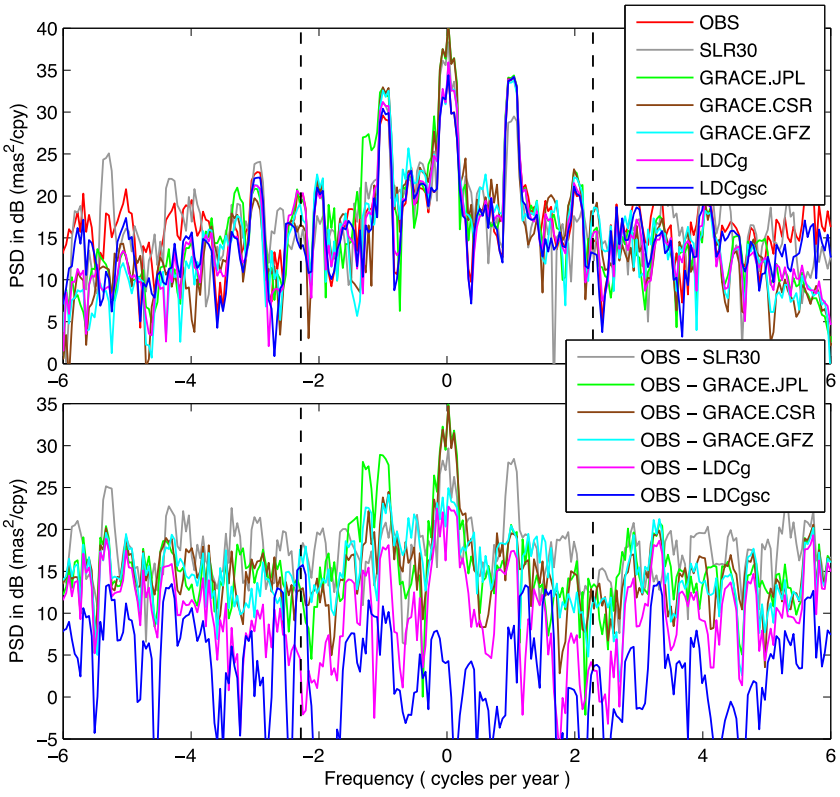

(a)

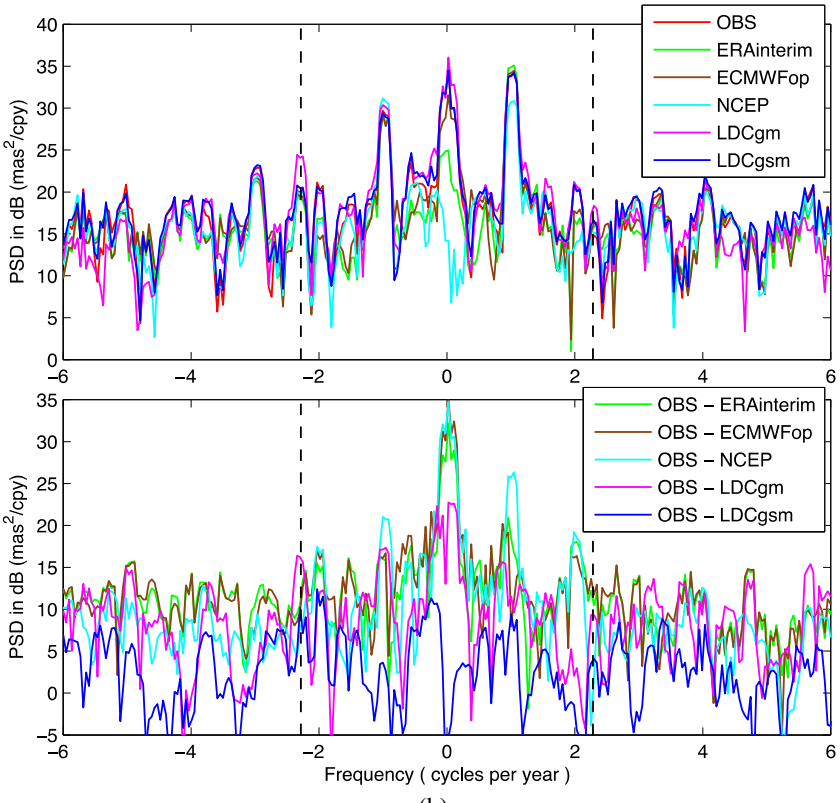

(b)

Fig. 4. PSD (Power spectrum density) comparisons among the geodetic and geophysical excitations. (a) For matter-term excitations derived from various GRACE/SLR potential coefficients and the LDCgsc solution (Top), and for the corresponding excess excitations (Bottom). (b) For geophysical excitations derived from various meteorological models and the LDCgsm solution (Top), and for the corresponding excess excitations (Bottom). One can see obvious ±2.3 cpy (marked with dashed black lines) signals in all GRACE data and the LDCg solution. The excess excitations corresponding to LDCg and LDCgsm are reduced significantly at all frequencies.

Table 4
Standard derivations of the excess excitations (unit: mas). Here "matter only" means only matter term excitations are considered, "matter + motion" means both matter and motion terms are considered, and SD(x) means the standard derivation of x. Note that SD (χ_{OBS}) = 37.4559 mas.

Matter only		Matter + motion	
$SD(\chi_{OBS}-\chi_{SLR30})$	30.8390	$SD(\chi_{OBS}-\chi_{ERAinterim})$	20.4115
$SD(\chi_{OBS}-\chi^{JPL}_{GRACE})$	32.7759	$SD(\chi_{OBS}-\chi_{ECMWFop})$	26.0715
$SD(\chi_{OBS}-\chi^{CSR}_{GRACE})$	29.5118	$SD(\chi_{OBS}-\chi_{NCEP})$	24.5974
$SD(\chi_{OBS}-\chi^{GFZ}_{GRACE})$	22.7640		
$SD(\chi_{OBS}-\chi_{LDCg})$	14.8985	$SD(\chi_{OBS}-\chi_{LDCgm})$	12.5177
$SD(\chi_{OBS}-\chi_{LDCgsc})$	7.3598	$SD(\chi_{OBS}-\chi_{LDCgsm})$	5.4849

with higher frequencies, however, the case is reversed: the GRACE data present strong ~±2.3 cpy anomalies (their cause(s) is (are) not quite certain yet; see Appendix B for some discussions), and show obvious power losses near their Nyquist frequencies; the SLR data are also dominated by the strong noises due to the general problem of separating the various gravity field harmonics in the presence of orbit errors, which are in turn the result of imperfect dynamical models, imperfect geographic sampling due to a limited SLR network, and observational errors (though the ranging data errors should not be the limiting factor). On the contrary, meteorological data agree well with the geodetic excitation for these seasonal bands, implying seasonal changes in atmosphere, oceans and land water are relatively well modeled.

As to the GRACE-based matter-term excitations, we can find from Fig. 1 and 3 as well as Table 4 that the trend of GFZ series agrees best with the geodetic excitation and LDCgsc, while those for JPL and CSR are a bit overestimated. As to periodic components, the performances of CSR and GFZ series are comparable with each other, and both better than the JPL version.

The above show the reasons why not only GRACE + SLR data but also GCM outputs are needed to improve atmospheric, oceanic and hydrological/cryospheric excitations.

The benefits of our method are as follows:

1. Avoiding the above-mentioned steps introduced by GAC model to GSM data since we have used GSM + GAC, which is what GRACE satellites really measure.
2. Avoiding the errors introduced by GAC data derived from the ECMWF and OMCT operational runs, which are not quite reliable as shown by Chen et al. [5] and Fig. 2 of this study.
3. Recognizing the fact that meteorological matter terms χ_{matter} are much better than motion terms χ_{motion}. We have not subtracted χ_{motion} from the geodetic excitation χ_{obs} as done in previous studies [21], where the accuracy of χ_{obs} is significantly degraded by the poorly modeled χ_{motion} according to the law of error propagation. In addition, $\chi_{obs}-\chi_{motion}$ is not really χ_{matter} as assumed by them, but in fact $\chi_{matter}+\chi_{excess}$ since $\chi_{obs}=\chi_{matter}+\chi_{motion}+\chi_{excess}$, where the excess excitation χ_{excess} is even stronger than χ_{motion} (one can check that χ_{motion} (AE + OE) has the amplitude ~10 to 15 mas, while χ_{excess} ~20 mas except for the excess excitation corresponding to χ^{LDCgsm}; see Fig. 2 and Chen et al. [5] for more details).
4. Guaranteeing the conservation of global mass for the LDCgsm meteorological excitations, while the law is often violated for the original meteorological model data [15].

5. Discussions and conclusions

In this study, we have used various GRACE and SLR time series of (C_{21}, S_{21}) and various atmospheric, oceanic and hydrological model outputs to construct the optimized solution LDCgsm, relying on the LDC method proposed by Chen et al. [5] and the polar motion observations as general constraints. Absorbing the best components from GRACE/SLR data and model outputs, the LDCgsm solution can reveal not only periodic fluctuations but also secular trends in AAM, OAM and HAM/CAM, presents overwhelming advantage in both time and frequency domains with respect to the original model-based AAM, OAM and HAM, and significantly reduces the unexplained excitation from ~20 to 26 mas to ~5 mas (standard derivation value).

On the other hand, one may note that our results differ obviously from previous studies by e.g., Nastula et al. [21], which used $\chi_{obs}-\chi_{motion}$ to compare with χ_{matter}. However, due to uncertainties in the polar motion observations, GRACE and SLR data and meteorological models, $\chi_{obs}=\chi_{matter}+\chi_{motion}+\chi_{excess}$ and one can easily find that the seasonal components of χ_{excess} are even stronger than χ_{motion} (see Subsection 4.3 for details). Thus, it is misleading to compare $\chi_{obs}-\chi_{motion}$ and χ_{matter} directly as $\chi_{obs}-\chi_{motion}=\chi_{matter}+\chi_{excess}$ is stronger than χ_{matter} alone. In addition, as is well known (also see Chen et al. [5] and Section 4), χ_{motion} is much more uncertain than χ_{matter} and therefore $\chi_{obs}-\chi_{motion}$ contains larger error than χ_{matter} according to the law of error propagation. It is also unreasonable to constrain χ_{matter} using the less-accurate $\chi_{obs}-\chi_{motion}$. To conclude, the results obtained by this study are much more reliable than previous studies.

Based on the above reasons, we suggest using the LDCgsm AAM, OAM and HAM/CAM, rather than the original model-based ones or the GRACE/SLR based ones, to study polar motion excitations, which helps to gain more reliable results. It also helps to study polar motion excited by other causes by removing the LDCgsm AAM, OAM and HAM/CAM from the geodetic excitation.

Acknowledgments

Dr. Richard S. Gross kindly provided the updated ECCO kf80g data and helpful suggestions. Dr. John C. Ries provided helpful details and discussions about the SLR and GRACE data. Dr. Hao Ding helped checking the 2.3 cpy signals. This study is supported in parts by the National 973 Project of China (No. 2013CB733301 and 2013CB733305), the National Natural Science Foundation of China (No. 41474022, 41210006 and 41374022), the R&D Special Fund for Public Welfare Industry (Surveying and Mapping, No. 201512001), the Fundamental Research Funds for the Central Universities of China (No. 2042016kf0146), and the China Postdoctoral Science Foundation (No. 2014T70737). The LDCgsm meteorological excitation data are available upon request from Wei Chen (wchen@sgg.whu.edu.cn).

Appendices

A. Differences between various atmospheric, oceanic and hydrological model outputs

Several versions of the AAM, OAM and HAM time series are calculated on the basis of models for numerical weather prediction developed at various institutes. The theories, numerical methods and assumptions adopted by the different institutes sometimes differ, so their global atmospheric, oceanic and hydrological model results are not identical (see Table 2 and the following discussions for some examples). In addition, concerning the combined effects of atmospheric, oceanic and hydrological excitations (AE, OE and HE, respectively), we cannot simply add arbitrary versions of OE and HE to a certain AE since consistency among these atmospheric, oceanic and hydrological models would not be ensured. That is, the models of the ocean and hydrology should be the ones driven by outputs from the same atmosphere model [5]. Artificial signals might be introduced if modeling consistency is not enforced.

The NCEP/NCAR (hereafter NCEP for short) atmosphere model is based on the expressions of conservation of mass, momentum,

energy and moisture; however, the momentum equations are replaced by the vorticity and divergence equations to take advantage of the spectral technique in the horizontal [45], thus eliminating the difficulties associated with the spectral representation of vector quantities on a sphere [46]. The ECMWF atmosphere model is based on similar or equivalent prognostic equations (see Table A1). The most notable theoretical difference between the two models lies in the diagnostic equations giving the static relation between different model parameters: The NCEP model use the vertical velocity equation obtained from the continuity equation discretized in the vertical, while the ECWMF model use the gas law providing the relation between pressure, density and temperature.

Based on the MIT-GCM (Massachusetts Institute of Technology – General Circulation Model), the ECCO ocean model run at JPL is driven by the surface wind stress, heat and freshwater fluxes (but no surface pressure) from the NCEP reanalysis; the NCEP hydrological model is also driven by the outputs of the NCEP atmosphere model, and thus both the ECCO ocean model and the NCEP hydrological model are consistent with the NCEP atmosphere model. Among the different versions of the ECCO data, here we adopt the output of the kf80 run which has assimilated sea surface height data and removed the tidal contamination present in previous versions of the ECCO data (see Gross [41] for details).

Since the ECCO model is not forced by atmospheric surface pressure, it is common to assume the inverted barameter (IB) model to account for the effects of atmospheric pressure over the oceans when using the ECCO ocean model [Gross, 2010, personal communication]. The IB model is a realistic approximation of the oceans' response to surface pressure variations at long periods, but is generally thought to break down somewhere between a few and 10 days and is not valid at short periods such as 1–2 days [e.g., Wunsch and Stammer, 1997 [47]; Gross, 2010, personal communication].

The oceanic and continental hydrological mass transports are generated with the OMCT and the LSDM models using atmospheric forcing data from the ECMWF. The three models are “combined to ensure mass conserving freshwater fluxes among the three subsystems atmosphere, oceans, and continental hydrosphere in order to represent a closed global hydrological cycle” [13]. The model system is forced with various ECMWF atmospheric data sets, such as the ERA-40 reanalysis, the ERA Interim and the operational outputs, and thus there are different versions of AAM, OAM and HAM derived from those models.

In contrast to the ECCO model, the OMCT model simulates the response to atmospheric freshwater, energy and momentum fluxes that include the effects of atmospheric pressure; that is, the OMCT responds dynamically to the atmospheric pressure [Dobslaw, 2012, personal communication]. Therefore, the OMCT model avoids the IB or NIB (non-IB) assumption and might, in principle, provide a better description of atmosphere-ocean interactions than the ECCO model. In sum, the ECCO and OMCT models are different not only because they are driven by different atmosphere models, but also due to the treatment of the IB/NIB problem and the assimilation of sea surface height data.

B. About the 2.3 cpy signals

In Fig. 4, the ±2.3 cpy anomalies, which are very close to the S_2 alias frequency (161-day period or 2.283 cpy [48,49]), are found in the GRACE GSM (C_{21}, S_{21}) series (or GRACE-based excitations; see Eq. (9) for their theoretical relation). Noting S_2 alias corresponds to the degree-2 order-2 harmonics, why the ±2.3 cpy anomalies in (C_{21}, S_{21}) are so close to the S_2 alias frequency? Can any reliable relation between them be found?

For solid tides, it is well known that:

Table A1
Comparisons between the NCEP/NCAR and the ECMWF atmosphere models.

	NCEP/NCAR[a]	ECMWF[b]
Diagnostic equations	Hydrostatic equation	Hydrostatic equation
	Vertical velocity equation	**Gas law**
Prognostic equations	Thermodynamic equation	Thermodynamic equation
	Surface pressure equation (derived from equation of continuity)	Equation of continuity (equivalent to conservation of mass)
	Conservation of moisture	Conservation of moisture
	Divergence equation	Equation of motion (equivalent to conservation of momentum)
	Vorticity equation	

[a] http://www.emc.ncep.noaa.gov/gmb/wd23ja/doc/web2/chap2.html.
[b] Persson and Grazzini (2007) [15].

order $m = 0 \rightarrow$ long period tides (only affect C_{20})
order $m = 1 \rightarrow$ diurnal tides (only affect C_{21}, S_{21})
order $m = 2 \rightarrow$ semidiurnal tides (only affect C_{22}, S_{22})

Then S_2 alias is not expected to have anything to do with anomalies in (C_{21}, S_{21}).

However, for ocean tides, things are much more complicated, as there are coastlines which will change the tidal motions of the oceans, and then the above may not hold. An obvious example is the polar motion excited by long period ocean tides, where the degree-2 zonal tide generating potentials cause the tesseral oceanic mass changes and thus tidal polar motion (see e.g., Ch.8 of IERS Conventions 2010 [50]). So in a similar way, the ocean tide S_2 might cause changes in (C_{21}, S_{21}) and thus tidal polar motion. Then there would be S_2 alias in (C_{21}, S_{21}) if ocean tides are not completely removed. According to its spatial distributions as shown by the plots in Seo et al., [49], the S_2 alias due to errors in ocean tide models can contribute to harmonics with different orders and degrees, not limiting to (C_{21}, S_{21}).

In addition, Griffiths and Ray [51] once did an empirical study on the effects of subdaily EOP (Earth Orientation Parameter) tide model errors on IGS product results, and found the EOP series are affected at both long and short periods and in very complicated non-intuitive ways. Then if GPS tracking data are used in the GRACE data analyses, the S_2 alias might present because GPS orbits are very nearly resonant with the S_2 period.

On the other hand, John C. Ries and Minkang Cheng (2015, personal communications) suggest that the 2.3 cpy signals in (C_{21}, S_{21}) is caused by a significant but unknown excitation that is dependent on the beta-angle of the GRACE orbit plane with respect to the Sun (which has the same periodicity). In addition, Cheng and Ries [52] tried to prove that ~161-day signal in C_{20} is not originated in the S2 tide alias.

By analyzing the matter and motion terms of AAMs, OAMs and HAMs (all sampled every 6 h) from the four data sets NCEP, ECMWFop, ERAinterim and LDCgsm, Wei Chen found all data support that there are strong ~161-day signals in the AAM matter and motion terms (OAMs and HAMs have no (or very weak) such signals). The 161-day variations in atmospheric pressure and wind may also impact the GRACE twin satellites and thus the GRACE data.

To conclude, we may need more sound clues to check the causes of the 2.3 cpy signals in (C_{21}, S_{21}), which might be a tough task covering many fields.

References

[1] T.M. Eubanks, Variations in the orientation of the Earth, in: D.E. Smith, D.L. Turcotte (Eds.), Contributions of Space Geodesy to Geodynamics: Earth Dynamics, Geodyn. Ser., vol. 24, AGU, Washington, D. C., 1993, pp. 1–54.

[2] S.R. Dickman, Evaluation of “effective angular momentum function” formulations with respect to core-mantle coupling, J. Geophys. Res. 108 (B3) (2003) 2150, http://dx.doi.org/10.1029/2001JB001603.
[3] R.S. Gross, Earth rotation variations – long period, in: 2nd ed., in: Gerald Schubert (Ed.), Treatise on Geophysics, vol. 3, Elsevier, New York, 2015, pp. 215–261.
[4] W. Chen, J. Ray, J.C. Li, C. Huang, W. Shen, Polar motion excitations for an Earth model with frequency-dependent responses: 1. A refined theory with insight into the Earth's rheology and core-mantle coupling, J. Geophys. Res. Solid Earth 118 (2013a) 4975–4994, http://dx.doi.org/10.1002/jgrb.50314.
[5] W. Chen, J. Ray, W. Shen, C. Huang, Polar motion excitations for an Earth model with frequency-dependent responses: 2. Numerical tests of the meteorological excitations, J. Geophys. Res. Solid Earth 118 (2013b) 4995–5007, http://dx.doi.org/10.1002/jgrb.50313.
[6] J.M. Wahr, The effects of the atmosphere and oceans on the Earth's wobble – I. Theory, Geophys. J. R. Astron. Soc. 70 (1982) 349–372.
[7] J.M. Wahr, The effects of the atmosphere and oceans on the Earth's wobble – II. Results, Geophys. J. R. Astron. Soc. 74 (1983) 451–487.
[8] B.F. Chao, A.Y. Au, Atmospheric excitation of the Earth's annual wobble: 1980–1988, J. Geophys. Res. 96 (B4) (1991) 6577–6582.
[9] M. Thomas, Ocean Induced Variations of Earth's Rotation – Results From a Simultaneous Model of Global Circulation and Tides (PhD thesis), Univ. of Hamburg, Hamburg, Germany, 2002, 129 pp.
[10] R. Dill, Hydrological Model LSDM for Operational Earth Rotation and Gravity Field Variations, Scientific Technical Report STR08/09, GFZ Potsdam, Germany, 2008.
[11] A. Brzeziński, J. Nastula, B. Kołaczek, Seasonal excitation of polar motion estimated from recent geophysical models and observations, J. Geodyn. 48 (2009) 235–240.
[12] C. Bizouard, L. Seoane, Atmospheric and oceanic forcing of the rapid polar motion, J. Geod. 84 (2010) 19–30, http://dx.doi.org/10.1007/s00190-009-0341-2.
[13] H. Dobslaw, R. Dill, A. Grotzsch, A. Brzeziński, M. Thomas, Seasonal polar motion excitation from numerical models of atmosphere, ocean, and continental hydrosphere, J. Geophys. Res. 115 (2010) B10406, http://dx.doi.org/10.1029/2009JB007127.
[14] W. Bourke, A multi-level spectral model. I. Formulation and hemispheric integrations, Mon. Weather Rev. 102 (1974) 687–701.
[15] A. Persson, F. Grazzini, User Guide to ECMWF Forecast Products, 2007. Meteorological Bulletin M3.2. (user manuals).
[16] H. Yan, B.F. Chao, Effect of global mass conservation among geophysical fluids on the seasonal length of day variation, J. Geophys. Res. 117 (2012), B02401, http://dx.doi.org/10.1029/2011JB008788.
[17] L. Koot, O. de Viron, V. Dehant, Atmospheric angular momentum time-series: characterization of their internal noise and creation of a combined series, J. Geod. 79 (2006) 663–674.
[18] L.J. Neef, K. Matthes, Comparison of Earth rotation excitation in data-constrained and unconstrained atmosphere models, J. Geophys. Res. 117 (2012), D02107, http://dx.doi.org/10.1029/2011JD016555.
[19] M. Cheng, B.D. Tapley, Variations in the Earth's oblateness during the past 28 years, J. Geophys. Res. 109 (2004), B09402, http://dx.doi.org/10.1029/2004JB003028.
[20] M. Cheng, J.C. Ries, B.D. Tapley, Variations of the Earth's figure axis from satellite laser ranging and GRACE, J. Geophys. Res. 116 (2011), B01409, http://dx.doi.org/10.1029/2010JB000850.
[21] M. Cheng, B.D. Tapley, J.C. Ries, Deceleration in the Earth's oblateness, J. Geophys. Res. Solid Earth 118 (2013) 740–747, http://dx.doi.org/10.1002/jgrb.50058.
[22] J. Nastula, R.M. Ponte, D.A. Salstein, Comparison of polar motion excitation series derived from GRACE and from analyses of geophysical fluids, Geophys. Res. Lett. 34 (2007), L11306, http://dx.doi.org/10.1029/2006GL02893.
[23] F. Göttl, M. Schmidt, F. Seitz, M. Bloßfeld, Separation of atmospheric, oceanic and hydrological polar motion excitation mechanisms based on a combination of geometric and gravimetric space observations, J. Geod. 89 (2015) 377–390, http://dx.doi.org/10.1007/s00190-014-0782-0.
[24] H. Dobslaw, F. Flechtner, I. Bergmann-Wolf, Ch Dahle, R. Dill, S. Esselborn, I. Sasgen, M. Thomas, Simulating high-frequency atmosphere-ocean mass variability for dealiasing of satellite gravity observations: AOD1B RL05, J. Geophys. Res. Oceans 118 (2013) 3704–3711, http://dx.doi.org/10.1002/jgrc.20271.
[25] F. Flechtner, H. Dobslaw, E. Fagiolini, Gravity Recovery and Climate Experiment: AOD1B Product Description Document for Product Release 05 (Rev. 4.2), GRACE 327–750 (GR-GFZ-AOD-0001), 2014.
[26] R.T.H. Barnes, R. Hide, A.A. White, C.A. Wilson, Atmospheric angular momentum fluctuations, length-of-day changes and polar motion, Proc. R. Soc. Lond. Ser. A 387 (1983) 31–73, http://dx.doi.org/10.1098/rspa.1983.0050.
[27] D.A. Salstein, D.M. Kann, A.J. Miller, R.D. Rosen, The sub bureau for atmospheric angular momentum of the International Earth Rotation Service (IERS): a meteorological data center with geodetic applications, Bull. Am. Meteorol. Soc. 74 (1993) 67–80.
[28] R.S. Gross, I. Fukumori, D. Menemenlis, Atmospheric and oceanic excitation of the Earth's wobbles during 1980–2000, J. Geophys. Res. 108 (B8) (2003) 2370, http://dx.doi.org/10.1029/2002JB002143.
[29] Y.H. Zhou, D.A. Salstein, J.L. Chen, Revised atmospheric excitation function series related to Earth variable rotation under consideration of surface topography, J. Geophys. Res. 111 (2006), D12108, http://dx.doi.org/10.1029/2005JD006608.
[30] B.F. Chao, R.S. Gross, Changes in the Earth's rotation and low-degree gravitational field induced by earthquakes, Geophys. J. Roy. Astron. Soc. 91 (1987) 569–596.
[31] R.S. Gross, Correspondence between theory and observations of polar motion, Geophys. J. Int. 109 (1992) 162–170, http://dx.doi.org/10.1111/j.1365-246X.1992.tb00086.x.
[32] W. Chen, W.B. Shen, New estimates of the inertia tensor and rotation of the triaxial nonrigid Earth, J. Geophys. Res. 115 (2010) B12419, http://dx.doi.org/10.1029/2009JB007094.
[33] W. Chen, J.C. Li, J. Ray, W. Shen, C. Huang, Consistent estimates of the dynamical figure parameters of the Earth, J. Geod. 89 (2) (2015) 179–188, http://dx.doi.org/10.1007/s00190-014-0768-y.
[34] S.R. Dickman, Dynamic ocean-tide effects on Earth's rotation, Geophys. J. Int. 112 (1993) 448–470, http://dx.doi.org/10.1111/j.1365-246X.1993.tb01180.x.
[35] H. Ding, B.F. Chao, Solid pole tide in global GPS and superconducting gravimeter observations: signal retrieval and inference for mantle anelasticity, Earth Planet. Sci. Lett. 459 (2017) 244–251.
[36] W.A. Heiskanen, H. Moritz, Physical Geodesy, W. H. Freeman, San Francisco, Calif, 1967.
[37] E. Groten, Fundamental parameters and current (2004) best estimates of the parameters of common relevance to astronomy, geodesy, and geodynamics, J. Geod. 77 (2004) 724–797, http://dx.doi.org/10.1007/s00190-003-0373-y.
[38] W. Chen, J. Ray, J.C. Li, Theory for polar motion: error analyses and potential refinements to the accuracy level of geodetic observations, in: Presented at the IAG Commission 1 Symposium 2014 – Reference Frames for Applications in Geosciences (REFAG2014), Kirchberg, Luxembourg, 13–17 Oct 2014, 2014.
[39] C. Bizouard, D. Gambis, The combined solution C04 for Earth orientation parameters consistent with international terrestrial reference frame 2005, IAG Symp. 134 (2009) 265–270, http://dx.doi.org/10.1007/978-3-642-00860-3_41.
[40] E. Fagiolini, F. Flechtner, M. Horwath, H. Dobslaw, Correction of inconsistencies in ECMWF's operational analysis data during de-aliasing of GRACE gravity models, Geophys. J. Int. 202 (2015) 2150–2158.
[41] J. Wahr, R.S. Nerem, S.V. Bettadpur, The pole tide and its effect on GRACE time-variable gravity measurements: implications for estimates of surface mass variations, J. Geophys. Res. Solid Earth 120 (2015) 4597–4615, http://dx.doi.org/10.1002/2015JB011986.
[42] R.S. Gross, An improved empirical model for the effect of long period ocean tides on polar motion, J. Geod. 83 (2009) 635–644, http://dx.doi.org/10.1007/s00190-008-0277-y.
[43] Y. Mireault, J. Kouba, J. Ray, IGS Earth rotation parameters, GPS Solutions 3 (1) (1999) 59–72.
[44] J. Ray, J. Griffiths, X. Collilieux, P. Rebischung, Subseasonal GNSS positioning errors, Geophys. Res. Lett. 40 (2013a) 5854–5860, http://dx.doi.org/10.1002/2013GL058160.
[45] J. Ray, P. Rebischung, R. Schmid, Dependence of IGS products on the ITRF datum, in: Z. Altamimi, X. Collilieux (Eds.), Reference Frames for Applications in Geosciences, IAG Symposia, vol. 138, Springer-Verlag, 2013b, pp. 63–67, http://dx.doi.org/10.1007/978-3-642-32998-2_11.
[46] B. Machenhauer, E. Rasmussen, On the Integration of the Spectral Hydrodynamical Equations by a Transform Method, Institute for Theoretical Meteorology, University of Copenhagen, Copenhagen, Denmark, 1972. Report No. 3.
[47] C. Wunsch, D. Stammer, Atmospheric loading and the oceanic “inverted barometer” effect, Rev. Geophys. 35 (1997) 79–107.
[48] R.D. Ray, D.D. Rowlands, G.D. Egbert, Tidal models in a new era of satellite gravimetry, Space Sci. Rev. 108 (2003) 271–282.
[49] K.W. Seo, C.R. Wilson, S.C. Han, D.E. Waliser, Gravity Recovery and Climate Experiment (GRACE) alias error from ocean tides, J. Geophys. Res. 113 (2008) B03405, http://dx.doi.org/10.1029/2006JB004747.
[50] G. Petit, B. Luzum (Eds.), IERS Conventions (2010), IERS Technical Notes 36, Verlag des BundesamtsfürKartographie und Geodäsie, Frankfurt am Main, 2010. ISBN: 3-89888-989-6; 179 pp.
[51] J. Griffiths, J. Ray, Sub-daily alias and draconitic errors in the IGS orbits, GPS Solut. 17 (2013) 413–422, http://dx.doi.org/10.1007/s10291-012-0289-1.
[52] M. Cheng, J.C. Ries, The unexpected signal in GRACE estimates of C20, J Geod (2017), http://dx.doi.org/10.1007/s00190-016-0995-5 (in press).

Wei Chen, Wuhan University, Luoyu Road 129, Wuhan, Hubei, China, email: weichen.geo@gmail.com **Current position** Associate Professor, School of Geodesy and Geomatics, Wuhan University, Wuhan, China **Educations** 12/2011, PhD in Solid Geophysics, Wuhan University6/2008, Master in Solid Geophysics, Wuhan University6/2006, Bachelor in Geophysics, Wuhan University **Research interests** Earth rotation theory (for nutation, polar motion and length-of-day variation) and its application;Frequency-dependent responses in the Earth rotation dynamics (modeling the frequency dependences of Love numbers);Meteorological excitation of nutation/polar motion/length-of-day variation;Time-variable gravity.